IEEE Robotics and Automation Letters (RA-L) paper, presented at ICRA 2024, Yokohama, Japan. Cite as RA-L paper.

Design and Validation of Soft Sliding Structure with Adjustable Stiffness for Ankle Sprain Prevention

Seoyeon Ham[1,2], Soe Lin Paing[2], Brian Byunghyun Kang[3,*], Hyunglae Lee[2,*], and Wansoo Kim[4,*]

***Abstract*—This study presents the design and validation of a soft sliding stiffness structure with a soft-rigid layer sliding mechanism. It aims to mitigate ankle sprains and address the progression of chronic ankle instability by providing stiffness support. The soft-rigid layer sliding mechanism of the structure is designed to achieve a wide range of stiffness while maintaining a compact form factor. The structure incorporates rigid retainer pieces within each layer, which allows for sliding within a hollow cuboid structure and enables modulation of stiffness. An analytical model is presented to investigate the variations in stiffness resulting from the different sliding states. The stiffness characteristics of the structure were validated through both bench tests and human subject tests. The gradual sliding of the structure's layer resulted in an increase in stiffness, aligning with the analytical model's predictions. At the most rigid stage (0% alignment), the stiffness exhibited a significant increase of 111.1% compared to the most flexible stage (100% alignment). Additionally, the human subject testing demonstrated a stiffness increase of up to 93.8%. These results underscore the potential applicability of the soft sliding structure in ankle support applications.**

***Index Terms*—Soft sensors and actuators, soft robot applications, wearable robotics.**

I. Introduction

ANKLE sprains are prevalent musculoskeletal injuries that affect a significant number of individuals [1], [2]. Risk factors for ankle sprains include previous ankle injuries, inadequate rehabilitation, and participating in high-impact sports. Certain intrinsic factors, such as joint laxity and muscle imbalances, can predispose individuals to ankle sprains [3], [4]. Moreover, the recurrence rate for ankle sprains is notably high, with many people experiencing subsequent injuries within one year of the initial event [5], [6]. Repeated ankle sprains can eventually lead to chronic ankle instability [7].

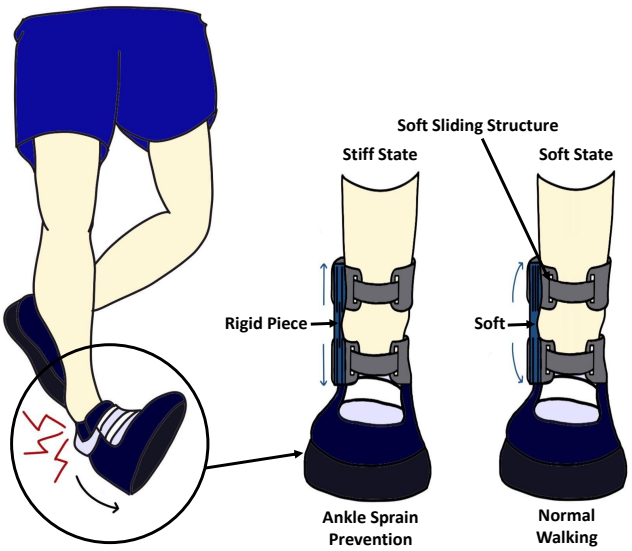

Fig. 1. Illustration highlighting the importance of using an ankle brace with a soft sliding structure for the prevention of ankle sprains in everyday activities. The soft sliding structure is integrated into the side of the ankle brace, enabling the adjustment of ankle stiffness from soft state to stiff state by sliding the soft-rigid layer.

External support has proven to be an effective proactive method for preventing ankle sprains [8]–[10]. This involves utilizing aids such as taping and braces to provide support to the ankle and enhance its stability [11], [12]. Taping uses kinesiology tapes to provide external support. However, it can be time-consuming and often requires professional assistance for proper application [13]. Ankle braces have also gained widespread use to address the aforementioned limitation. However, despite their improvement, braces still have the limitation of providing a uniform level of support without considering an individual's unique ankle conditions. As ankle sprains can occur in various situations with varying degrees of severity, it becomes crucial to provide ankle braces with adjustable or customizable stiffness support to effectively meet the specific needs of each individual [2], [14]–[16].

To address this issue, a recent study introduced a variable stiffness actuator, known as the Multi-material Actuator for Variable Stiffness (MAVS). This actuator is pneumatically driven to adjust stiffness by varying air pressure within it [17]. It supports inversion and eversion of the ankle in the frontal plane without impacting natural ankle motion in the sagittal plane [18]. However, using a pneumatic actuator necessitates

Manuscript received: August, 2, 2023; Revised October, 29, 2023; Accepted November, 26, 2023.

This paper was recommended for publication by Editor C. Laschi upon evaluation of the Associate Editor and Reviewers' comments. This work was supported by the National Research Foundation of Korea (NRF) grant funded by the Korea government (Ministry of Science and ICT) (No. 2022R1C1C1008306), and the National Institute of Arthritis and Musculoskeletal and Skin Diseases of the National Institutes of Health under Award Number R01AR080826.

[1]S. Ham is with Interdisciplinary Robot Engineering Systems Department, Hanyang University, 55, Hanyangdaehak-ro, Sangnok-gu, Ansan-si, Gyeonggi-do, Republic of Korea. hcpretty99@hanyang.ac.kr

[2]S. Ham, S. L. Paing, and H. Lee are with the the Neuromuscular Control and Human Robotics Laboratory in the Ira A. Fulton Schools of Engineering, Arizona States University, AZ, USA. spaing@asu.edu; hyunglae.lee@asu.edu

[3]B. B. Kang is with Intelligent Mechatronics Engineering Department, Sejong University, Seoul, Republic of Korea.brianbkang@sejong.ac.kr

[4]W. Kim is with Robotics Department, Hanyang University ERICA, Ansan-si, Gyeonggi-do, Republic of Korea. wansookim@hanyang.ac.kr

Digital Object Identifier (DOI): see top of this page.

IEEE Robotics and Automation Letters (RA-L) paper, presented at ICRA 2024, Yokohama, Japan. Cite as RA-L paper.

IEEE Robotics and Automation Letters (RA-L) paper, presented at ICRA 2024, Yokohama, Japan. Cite as RA-L paper.

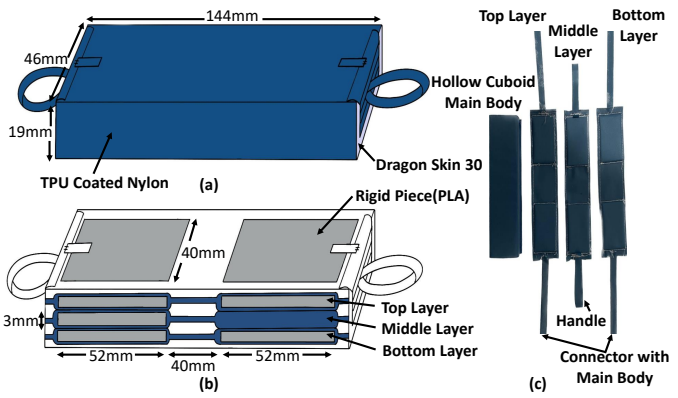

Fig. 2. Design of the soft sliding structure. (a) The outer part design of the structure. (b) The internal components of the structure. (c) The main components of the structure consisting of main body and the three soft-rigid layers.

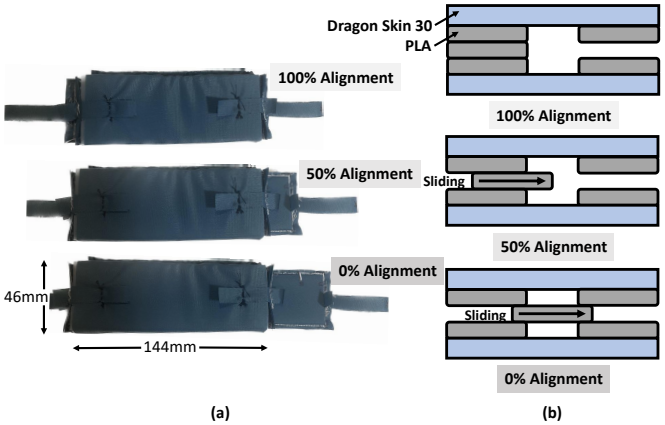

Fig. 3. Soft-rigid layer sliding mechanism of the soft sliding structure. (a) 100, 50, and 0% alignment stages of the soft sliding structure. (b) A side-view illustration explaining the operation of the soft-rigid layer sliding mechanism.

carrying an air pump to generate the required pressure, which can be inconvenient. Additionally, achieving precise control with pneumatic actuators can be challenging. In response to these challenges, an adjustable stiffness actuator using a soft-rigid combined layer jamming mechanism was developed in previous research [19]. This mechanism allowed for a gradual transition from an unjammed to a jammed state, addressing some of the limitations of the existing MAVS technologies. However, using multiple layers to demonstrate the various stages of stiffness resulted in a bulky design for practical ankle attachment.

Building upon the insights from the previous studies, the current study introduces a soft sliding structure design that incorporates a soft-rigid layer sliding mechanism. These soft sliding structures are intended for attachment using ankle brace that will be worn over the ankle (Fig. 1). The structure includes rigid retainer pieces within each layer, enabling smooth sliding within a hollow cuboid structure and allowing for modulation of stiffness at different sliding stages. An analytical model is developed to establish a theoretical foundation for the structure's soft-rigid layer sliding mechanism. The efficacy of the proposed soft sliding structure is thoroughly validated through comprehensive testing, including bench testing and human subject testing. This validation process aims to assess the structure's performance and effectiveness in real-world scenarios.

The remainder of this paper, which mainly focused on the design of soft sliding structure and validation of soft-rigid layer sliding mechanism, is organized as follows: Section II provides a detailed design and analytical modeling of the proposed soft sliding structure. Section III presents the experimental validation of the structure with bench testing and human subject testing. Finally, Section IV discusses the results and potential future work.

II. Design and Analytical Modeling of Soft Sliding Structure

A. Design of Soft Sliding Structure

The primary design objective of the soft sliding structure is to have a wide stiffness range using a rigid retainer piece, while allowing for stiffness changes. Unlike the previous study [19], stiffness change is implemented by sliding the layer without adding layers. Thus the overall volume can be minimized compared to the soft-rigid combined layer jamming mechanism. Furthermore, the soft-rigid layer sliding mechanism addressed the limitations of other similar mechanisms that use soft-rigid combined materials. In the work of Park *et al.*, layers are arranged horizontally in a row to implement dual stiffness with sliding mechanism [20]. However, the width of the human ankle is too narrow to arrange the layers horizontally. To address this, soft-rigid layer sliding mechanism was implemented by stacking a total of three layers vertically. In the work of Thalman *et al.*, pneumatic mechanism was used by inserting a rigid piece into an actuator [17]. Although it is a similar study that reduces volume using rigid pieces, soft-rigid layer sliding mechanism has the advantage of being able to operate without using a pneumatic pump.

The soft sliding structure consists of a hollow cubic structure constructed using Dragon Skin 30 material, known for its flexibility, and covered with a layer of thermoplastic polyurethane (TPU) coated nylon fabric (200 Denier Rockywoods Fabrics) (Fig. 2(a)). Inside this structure, three distinct layers are present, with each containing rigid pieces made of Polylactic Acid (PLA) material (Fig. 2(b)). To form a single layer, the rigid pieces, separated from each other, are wrapped in TPU coated nylon fabric. However, in the middle layer, only one rigid piece is utilized. This is because the exposed rigid piece of the middle layer, when the structure slides, can make the user uncomfortable. The top and bottom layers are securely fixed to the main body using a connector, while the middle layer is designed to slide and move between the two

IEEE Robotics and Automation Letters (RA-L) paper, presented at ICRA 2024, Yokohama, Japan. Cite as RA-L paper.

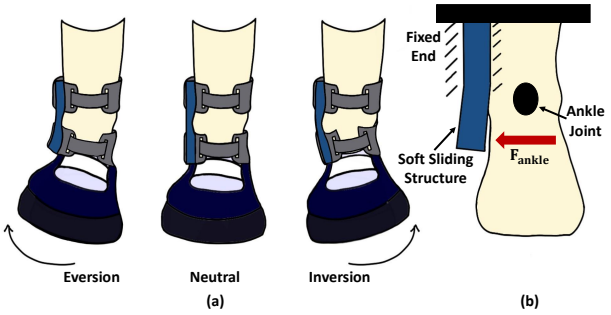

Fig. 4. Concept of anchoring the soft sliding structures to prevent ankle sprain. (a) Placement of the soft sliding structures on the side of the ankle joint, providing support for ankle movements in three positions: inversion, eversion, and neutral. (b) The anchoring of the soft sliding structure at one end and the structure being bent by the F_{ankle} force at the other end.

fixed layers, allowing for adjustment of alignment that results in varying stiffness levels (Fig. 2(c)).

The soft sliding structure has continuous alignment stages within the 0% to 100% alignment range, with the alignment degree tunable through the soft-rigid layer sliding mechanism. The purpose of the soft sliding structure is to provide adjustable stiffness support to the ankle. We focused on three alignment stages based on the stiffness values of the soft sliding structure that showed meaningful differences when considering the variability of human ankle stiffness [21], [22]. The stiffness values of the soft sliding structure associated with these alignment stages were initially derived from analytical modeling. Three stages are defined as follows and can be seen in Fig. 3:

- **100% alignment**: The rigid pieces are fully overlapped, and all layers are completely aligned. This represents the least rigid state of the structure (top of Fig.3).
- **50% alignment**: The middle layer moves halfway between the gaps of the rigid pieces. This results in a moderate level of rigidity (middle of Fig.3).
- **0% alignment**: The gap between the rigid pieces is reduced to zero, leaving no space between them. This stage makes the soft sliding structure becomes the most rigid and resistant to bending when an external force is applied (bottom of Fig.3).

B. Analytical Modeling of Soft Sliding Structure

In this section, the procedure for calculating the stiffness changes at each stage is explained to demonstrate the effectiveness of the soft-rigid layer sliding mechanism used in the soft sliding structure. The soft sliding structure is designed to anchor on the side of the ankle to provide support in inversion and eversion (Fig. 4(a)). When positioning the soft sliding structure, its center should be aligned with the center of the lateral malleolus. Furthermore, one side of the structure is fixed while the F_{ankle} force acts on the other side (Fig. 4(b)). Consequently, this can be visualized as a concentrated load P applied to the free end of a cantilever beam (Fig. 5).

To illustrate the stiffness changes at each stage, four different patterns of layer alignment are defined and denoted as colored boxes (Fig. 5):

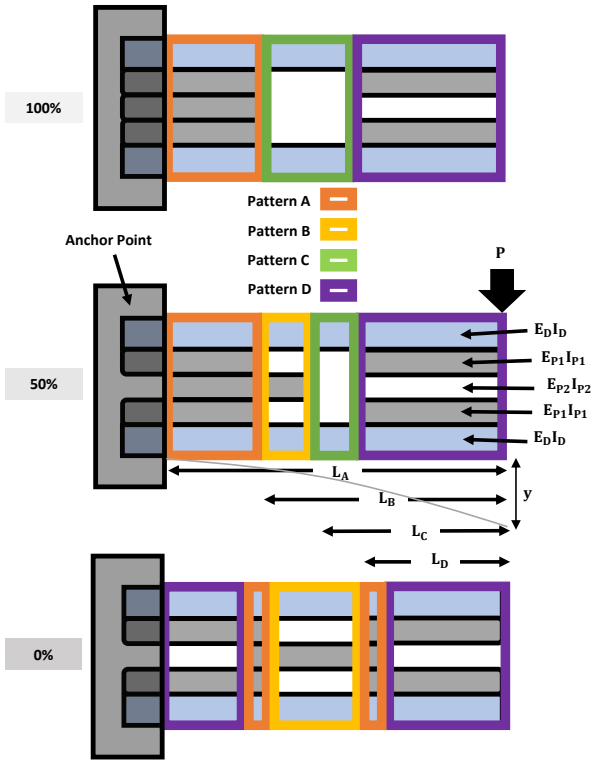

Fig. 5. Principle of the soft-rigid layer sliding mechanism at 100,50, 0% stages. When the soft sliding structure is anchored to the fixed end, four patterns denoted as A,B,C, and D, can be made in structure.

- **Pattern A (Orange; 5 layers)**: Two layers made with Dragon Skin 30 and three layers made with PLA.
- **Pattern B (Yellow; 3 layers)**: Two layers made with Dragon Skin 30 and one middle layer made with PLA.
- **Pattern C (Green; 2 layers)**: Two layers made with Dragon Skin 30.
- **Pattern D (Purple; 4 layers)**: Two layers made with Dragon Skin 30 and top and bottom layers made with PLA.

Different stages of alignment are formed with different combinations of the pattern A, B, C, and D. As these patterns in the soft sliding structure are connected in series, the overall stiffness at each alignment stage is expressed as follows:

$$\frac{1}{K_{\text{A}}} + \frac{1}{K_{\text{C}}} + \frac{1}{K_{\text{D}}} = \frac{1}{K_{\text{Overall-100}}} \tag{1}$$

$$\frac{1}{K_{\text{A}}} + \frac{1}{K_{\text{B}}} + \frac{1}{K_{\text{C}}} + \frac{1}{K_{\text{D}}} = \frac{1}{K_{\text{Overall-50}}} \tag{2}$$

$$\frac{1}{K_{\text{D}}} + \frac{1}{K_{\text{A}}} + \frac{1}{K_{\text{B}}} + \frac{1}{K_{\text{A}}} + \frac{1}{K_{\text{D}}} = \frac{1}{K_{\text{Overall-0}}} \tag{3}$$

where $K_{\text{Overall-100}}$, $K_{\text{Overall-50}}$, and $K_{\text{Overall-0}}$ represent the overall stiffness of the structure at 100%, 50%, and 0% alignment stage, respectively. K_{A}, K_{B}, K_{C}, and K_{D} represent the stiffness in each pattern section.

The stiffness K of each pattern (i.e., K_{A}, K_{B}, K_{C}, and K_{D}, respectively) follows the formula for calculating the stiffness of a cantilever beam subjected to a concentrated load P at the free end as:

IEEE Robotics and Automation Letters (RA-L) paper, presented at ICRA 2024, Yokohama, Japan. Cite as RA-L paper.

$$P = \frac{3EI_{\text{int}}y}{L^3}, \quad K = \frac{3EI_{\text{int}}}{L^3} \tag{4}$$

where y represents the deflection of the soft sliding structure, and L represents the distance from load P force to each pattern section. EI_{int} represents the integrated flexural rigidity [23], which is the rigidity of the entire layer. Hence, it can be calculated as follows:

$$EI_{\text{int}} = \sum_{i=1}^{n} E_i I_i \tag{5}$$

where E_i is the young' modulus and I_i is the moment of inertia of i-th layer from the top. Since the outermost TPU coated nylon fabric of the structure is very thin, the structure is modelled assuming that it is made of only Dragon Skin 30 and PLA. The values required to obtain the integrated flexural rigidity are the young's modulus of Dragon Skin 30 (E_{D} = 9 MPa) and the young's modulus of PLA (E_{P} = 3600 MPa). Additionally, the moment of inertia for each layer needs to be calculated. The hollow cuboid-shaped main body (i.e., the blue part in Fig. 5) is a layer made of Dragon Skin 30, and the moment of inertia in this part is:

$$I_{\text{D}} = \frac{bh_{\text{D}}^3}{12} + \left[bh_{\text{D}} \Big(\frac{h_{\text{D}}}{2} + h_{\text{P}} + \frac{h_{\text{P}}}{2} \Big)^2 \right] \tag{6}$$

where b is the width of the structure, h_{P} is the height of the PLA layer, and h_{D} is the height of the Dragon Skin 30 layer. Similarly, the rigid layers (i.e., the gray part in Fig. 5) are made of PLA, and the moment of inertia for each layer is calculated as follows:

$$I_{\text{P1}} = \frac{bh_{\text{P}}^3}{12} + \left[bh_{\text{P}} \Big(\frac{h_{\text{P}}}{2} + \frac{h_{\text{P}}}{2} \Big)^2 \right] \tag{7}$$

$$I_{\text{P2}} = \frac{bh_{\text{P}}^3}{12} \tag{8}$$

where I_{P1} represents the moment of inertia of the middle layer, and I_{P2} represents the moment of inertia of the top and bottom layers. The moment of inertia varies because the distance from the middle of the structure to each layer differs, leading to the distinction between I_{P1} and I_{P2}.

To determine the stiffness of each pattern section, we need to calculate the corresponding integrated flexural rigidity for each pattern. Applying pattern A, B, C, and D to Eq. (5), it is derived as shown in Table I.

By substituting the corresponding integrated flexural rigidity and L value (i.e., L_{A}, L_{B}, L_{C}, and L_{D}, respectively) for each pattern into Eq. (4), the stiffness value for each pattern can be obtained. The stiffness value in pattern A is calculated as:

$$K_{\text{A}} = \frac{3EI_{\text{intA}}}{L_{\text{A}}^3} \tag{9}$$

The stiffness values for patterns B, C, and D can be obtained using the same method. As shown in Eq. (9), the stiffness value for each pattern is influenced by the integrated flexural rigidity of each pattern. The integrated flexural rigidity is influenced by the number of layers within each pattern and is directly proportional to stiffness. Consequently, $K_{\text{Overall-0}}$, consisting of a higher number of pattern A and a lesser number of pattern C, yields a higher stiffness value.

TABLE I
INTEGRATED FLEXURAL RIGIDITY BY PATTERN

Pattern A	$EI_{\text{intA}} = 2(E_{\text{D}}I_{\text{D}}) + 2(E_{\text{P}}I_{\text{P1}}) + E_{\text{P}}I_{\text{P2}}$
Pattern B	$EI_{\text{intB}} = 2(E_{\text{D}}I_{\text{D}}) + E_{\text{P}}I_{\text{P2}}$
Pattern C	$EI_{\text{intC}} = 2(E_{\text{D}}I_{\text{D}})$
Pattern D	$EI_{\text{intD}} = 2(E_{\text{D}}I_{\text{D}}) + 2(E_{\text{P}}I_{\text{P1}})$

III. EXPERIMENTAL VALIDATION OF SOFT SLIDING STRUCTURE

To validate the effectiveness of the soft sliding structure in providing adjustable stiffness support, two experiments were conducted. The dimensions of the soft sliding structure were carefully chosen considering the structure's application to the ankle. Various stiffness stages can be realized even if the size of the soft sliding structure changes. However, since it is not possible to manufacture a structure of different sizes each time according to the ankle joint size of everyone, a structure of one size considering the average of the ankle joint size was created. Since the structure is attached in the lateral direction of the ankle, the size of the lateral malleolus was considered [24], [25]. The dimensions of the soft sliding structure used in the experiment were as follows: length of 144 mm, width of 46 mm, and height of 19 mm. Additionally, the rigid piece with a length of 52 mm, width of 40 mm, and height of 3 mm was used inside the soft sliding structure.

Two different experiments were conducted. The first experiment involved a bench test, which allowed for the assessment of structure stiffness under controlled perturbation conditions. This also enabled a comparison with the predictions derived from the analytical model. The second experiment involved a human subject test, which aimed to evaluate the structure's performance when worn by a human subject.

A. Experiments

1) Bench Test: A bench test was conducted to evaluate the change in stiffness of the soft sliding structure when subjected to bending forces. A motorized force tester (MARK-10 ESM303) was utilized, with one end of the soft sliding structure securely anchored using a bench vise (Parallel Jaw Grip, Medium) to simulate the condition shown in Fig. 4(b), and the other end connected to the non-stretchable fabric hook of a force gauge (Model M5-05) (Fig. 6).

The stiffness measurement experiment involved applying a controlled bending force to the soft sliding structure while the force gauge of the motorized force tester moved vertically

IEEE Robotics and Automation Letters (RA-L) paper, presented at ICRA 2024, Yokohama, Japan. Cite as RA-L paper.

Fig. 6. Experimental setup for the bench test. The soft sliding structure is firmly clamped to a bench vise on one end, while the other end is attached to the hook of a force gauge, ensuring a stable and controlled bench test setup.

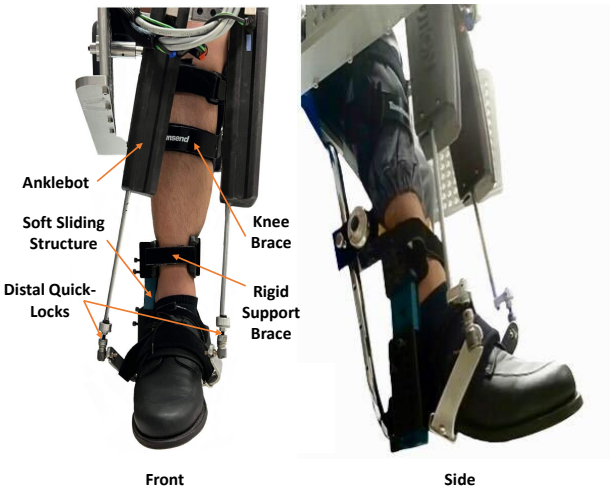

Fig. 7. Experimental setup for the human subject test. The subject wears a rigid support brace with a soft sliding structure securely anchored inside the bracket. To prevent knee movement, the subject also wears a knee brace, which is connected to the Anklebot. This setup ensures controlled conditions by limiting unwanted motion, allowing for a precise assessment of the soft sliding structure's effectiveness.

upwards. To ensure consistency across measurements, the force gauge was configured to move at a constant speed of 13 mm/min. The test began at the initial value of 0 mm on the force gauge and then progressively moved up to a displacement of 45 mm. This entire process was repeated for the three different stages of alignment, i.e., 100%, 50%, and 0% alignment stages.

2) Human Subject Test: A wearable ankle robot, Anklebot (Bionik, Inc.), was utilized to characterize ankle stiffness in the frontal plane [22] (Fig. 7). This robot was specifically designed to apply angular position perturbations to the ankle joint and record the corresponding torques, enabling the quantification of ankle stiffness. During the experiment, the subject wore a customized shoe and a knee brace while seated on a chair. The top part of the Anklebot was attached to the knee brace, and two end effectors of the structures were connected to a metal bracket attached to the bottom of the shoe. Additionally, a rigid support brace was employed to secure the soft sliding structure to the side of the human ankle. The rigid support brace was designed by considering the design of a specific shoe attached to the ankle robot. The soft sliding structure is anchored by aligning its center with the center of the subject's lateral malleolus and securing the top and bottom parts using the rigid support brace.

To evaluate the effect of the soft sliding structure on ankle stiffness, four different experimental conditions were examined: intrinsic (without the soft sliding structure), 100%, 50%, and 0% alignment stages. Angular position perturbations of 15 degree with speed of 5 deg/second were applied from the neutral ankle position, defined as the right angle between the shank and foot, in both inversion and eversion directions. Angular position perturbations were applied to the ankle 10 times in each of the four experimental condition for reliable stiffness quantification. The order of the experimental conditions was randomized. After every experimental condition, 10 minutes of rest was given. The experiment took approximately 2 hours to complete.

Ten healthy subjects (age: 21 - 32 years, gender: male, weight: 52 - 80 kg, height: 1.60 - 1.83 m) participated in the experiment. This study was approved by the Institutional Review Board of Arizona State University (STUDY00014244).

B. Data Analysis

1) Bench Test: The data analysis was conducted using real-time raw force measurements obtained from the force gauge through the MARK-10 software (MESUR®guage). Stiffness of the soft sliding structure was calculated by dividing the force measurements by deflection angle. Statistical significance across the alignment conditions was assessed using a one-way analysis of variance (ANOVA) test. Additionally, post-hoc multiple comparisons were conducted using the Tukey's Honestly Significant Difference tests.

2) Human Subject Test: The ankle angle and torque data were collected at a sampling frequency of 500 Hz and then filtered using the 4th order low-pass Butterworth filter with the cut-off frequency of 15 Hz. The ankle angle and torque data were isolated specifically for the static region in both the inversion and eversion directions. To quantify ankle stiffness, the average ankle angle and torque data were obtained from the extracted static region. Ankle stiffness was then calculated by simply dividing the mean torque by the mean ankle angle for each condition.

Since the Shapiro-Wilk test of normality indicated that the data was not normally distributed, Friedman test, a non-parametric equivalent to one-way repeated measure ANOVA test, was used to identify the difference between the testing conditions. For the post-hoc pairwise comparisons, the Wilcoxon sign rank test was used and p-values were adjusted using the Bonferroni correction method.

C. Results

1) Bench Test: The bench test results show the variation in stiffness of the soft sliding structure as the deflection angle

IEEE Robotics and Automation Letters (RA-L) paper, presented at ICRA 2024, Yokohama, Japan. Cite as RA-L paper.

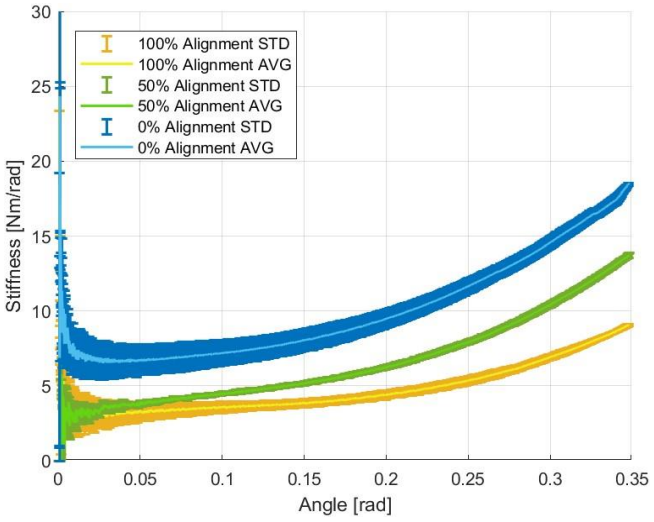

Fig. 8. Variation in stiffness of the soft sliding structure with the deflection angle at each alignment stage. Increasing the deflection angle and decreasing the alignment results in an increase in structure stiffness.

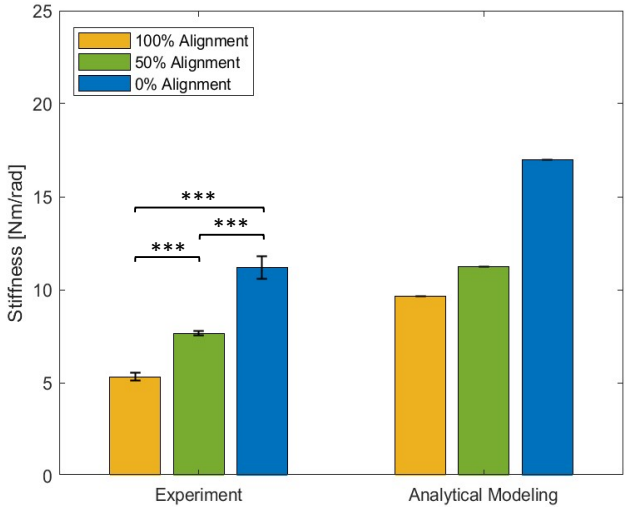

Fig. 9. Comparison of stiffness results between the bench test (Left) and analytical model (Right). An increasing trend in stiffness was consistently observed in both bench test and analytical model as the alignment decreased from 100 % to 0%. All pairwise comparisons reached the statistical significance of $p < 0.001$ (***).

increased up to 0.35 rad (Fig. 8). At the 100%, 50%, and 0% alignment stages, as the deflection increased, the stiffness increased with a small standard deviation of 0.60 Nm/rad or less. For deflection angles below approximately 0.08 rad, the stiffness values exhibited minimal variation. However, notable changes in stiffness were observed for each alignment stage when the deflection angle exceeded 0.08 rad.

When stiffness was evaluated for deflection angles exceeding 0.08 rad, a clear increasing trend was observed as the alignment decreased from 100% to 0% (Fig. 9 Left). Specifically, the stiffness at 50% and 0% alignment increased by 44.5% and 111.1% compared to the stiffness at 100% alignment, respectively. All pairwise comparisons exhibited statistically significant differences ($p < 0.001$), indicating a significant impact of alignment on the structure's stiffness. The increasing pattern of stiffness with decreasing alignment is consistent with the predictions from the analytical model (Fig. 9 Right). The analytical modeling results show that the stiffness at 50% and 0% alignment increased by 16.1% and 75.9%, respectively, compared to the stiffness at 100% alignment. The error between the experimental and analytical modeling results was 4.4 Nm/rad at 100%, 3.6 Nm/rad at 50%, and 5.8 Nm/rad at 0% alignment stage.

2) Human Subject Test: The results of the human subject test clearly demonstrate a significant effect of the soft sliding structure in increasing ankle stiffness. When compared to the without structure condition (i.e., intrinsic), stiffness increased by 6.8 Nm/rad in the 100% alignment stage. The stiffness gradually increased as the alignment decreased from 100% to 0% (Fig. 10). Relative to the intrinsic stiffness, the stiffness increased by 62.8% at 100% alignment, 76.2% at 50% alignment, and 93.8% at 0% alignment. The statistical analysis further confirms that all six post-hoc pairwise comparisons reached statistical significance. The Wilcoxon signed-rank test yielded an adjusted p-value = 0.012 for all pairwise comparisons.

To further evaluate the effect of the structure on ankle stiffness, offset stiffness was obtained by subtracting the intrinsic human ankle stiffness from the measured stiffness at each alignment stage. The results of the offset stiffness are well aligned with the results obtained from the bench test. The error between the offset stiffness in the human subject test and the measured stiffness in the bench test was 1.50, 1.24, and 0.02 Nm/rad at 100%, 50%, and 0% alignment stages, respectively.

In order to investigate the comfort level of the soft sliding structure when fixed on the ankle, a survey was conducted on 10 subjects who participated in the human subject test. In the survey, the subjects were asked to select one of five comfort levels they felt during the test. As shown in Fig. 11, all participants chose comfort Lv.3 or higher, ranging from comfort Lv.1 (very dissatisfied) to comfort Lv.5 (very satisfied). It is worth noting that 50% of the participants chose comfort Lv.5, 40% chose comfort Lv.4, and the remaining 10% chose Lv.3. In conclusion, the survey suggests that the soft sliding structure is comfortable when anchored to the ankle.

D. Discussion

While the experimental results of the bench test align with the trend predicted in the analytical model, some discrepancies were observed in the actual stiffness values. The primary source of discrepancies is thought to be the slippage between the layers forming the soft sliding structure, which was not accounted for in the analytical model. The discrepancies between the bench test and analytical modeling can be potentially minimized by applying tension to the sides of the layer. In addition, a notable limitation of the proposed stiffness calculation model is its assumption that there is no friction between the layers. Furthermore, the four patterns used in the analytical model might have oversimplified the actual

IEEE Robotics and Automation Letters (RA-L) paper, presented at ICRA 2024, Yokohama, Japan. Cite as RA-L paper.

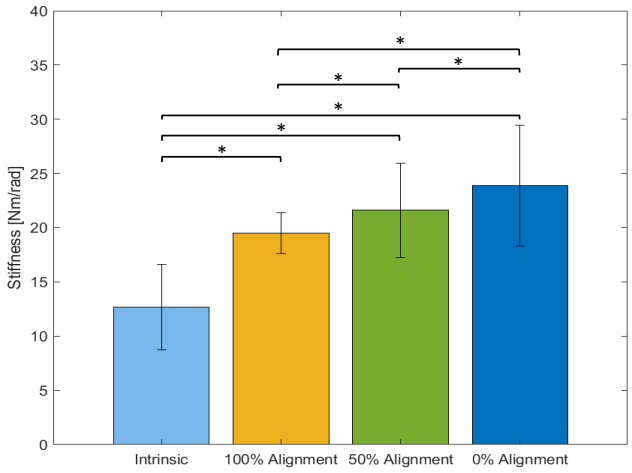

Fig. 10. Comparison of the ankle stiffness for different structure conditions in the human subject test. The stiffness significantly increased as the alignment decreased from 100% to 0%. All pairwise comparisons reached the statistical significance of adjusted $p < 0.05$ (*).

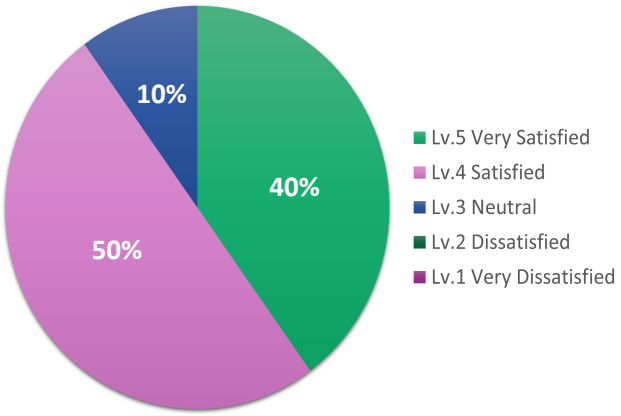

Fig. 11. Comfort level of the soft sliding structure when fixed on the ankle. Five comfort levels ranging from comfort Lv.1 (very dissatisfied) to comfort Lv.5 (very satisfied).

complicated interaction characteristics between the layers, potentially leading to errors. The analytical modeling could potentially be improved by considering the friction between layers and by providing a detailed subdivision of the area within the soft sliding structure, rather than oversimplifying the structure.

Compared to the error between the bench test and analytical model, the error between the bench test and human subject test was relatively small, which can be attributed to the differences in loading conditions. In the bench test, concentrated loading was applied to the one end of the structure while the other end was fixed. However, in the human subject test, the loading was distributed from the ankle to the area at the end of the structure, leading to variations in ankle stiffness characterization. Despite these discrepancies, the analytical modeling and two experiments consistently showed a sequential increase in stiffness from 100%, to 50%, and then to 0% alignment stage, confirming the adjustable stiffness capability of the soft sliding structure.

The experimental results support the potential use of the soft sliding structure to effectively prevent ankle sprain by offering a range of adjustable stiffness support to the ankle. A relevant study by Willwacher *et al.* demonstrated the benefits of an adaptive ankle sprain protection brace, which becomes active only when the ankle experiences significant deflection. This brace showed considerable improvements in active ankle range of motion, subjective comfort, and restriction ratings compared to conventional passive ankle braces [26]. Furthermore, in the work of Zinder *et al.*, the use of a lace-up and a semi-rigid brace resulted in an average increase in ankle stiffness of healthy subjects by 3.7 ± 0.7 Nm/rad and 7.5 ± 2.1 Nm/rad, respectively [27]. These stiffness values fall within the range of increase in ankle stiffness achievable by adjusting the alignment stages of the soft sliding structure. Thus, the soft sliding structure holds promise as a viable alternative to existing passive ankle braces for more effective prevention of ankle sprains.

Despite the promising results, the structure presented in this study has certain limitations. One limitation is that bending only occurs in the middle of the structure where the degree of alignment changes. Another limitation is that the manual adjustment of the alignment stages is required to change the structure stiffness, which can be cumbersome in practical use. These limitations need to be considered as a subject for future studies. Other limitation is that the human experiment was conducted with subjects seated. This controlled experimental setup allowed us to isolate and investigate the influence of the soft sliding structure on ankle stiffness while minimizing any potential effects at the physical interface between the device and the ankle. However, this effect might be pronounced during functional activities like standing or walking. To fully validate the effectiveness of the soft sliding structure, future study is warranted to investigate potential effects from the physical interface.

IV. Conclusion

This study introduced a soft sliding structure featuring a soft-rigid layer sliding mechanism, specifically designed for integration into the ankle. The structure incorporates rigid pieces within a hollow cuboid-shaped soft body, allowing it to achieve a range of adjustable stiffness. The concept of the soft sliding structure was validated through analytical modeling, and its effectiveness was further confirmed through both bench testing and human subject testing. Both experiments consistently demonstrated that the soft sliding structure's stiffness increased progressively in the order of 100%, 50%, and 0% alignment stages. This finding emphasizes the structure's capability to achieve varying levels of ankle stiffness by adjusting its alignment stages, setting it apart from existing ankle braces that offer fixed rigidity.

Future work will focus on automating the adjustment of alignment stages using an actuator. This is because actuation and control play a crucial role in supporting the practicality of the soft sliding structure's design in dynamic settings.

IEEE Robotics and Automation Letters (RA-L) paper, presented at ICRA 2024, Yokohama, Japan. Cite as RA-L paper.

Additionally, a durability test will be conducted to clarify whether the soft sliding structure remains stable on the ankle after repeated motions. The results of this test will be used to optimize the material selection for the soft sliding structure. Moreover, comfort level of the soft sliding structure when fixed on the ankle is an important aspect that should be investigated as part of our future work. Therefore, it is imperative to improve the design of the ankle brace from the current rigid design to a more human-friendly design by utilizing composite materials. Furthermore, a series of experiments and analysis will be carried out to investigate how different postures during normal activities such as standing or walking affect the performance of the soft sliding structure and user comfort.

REFERENCES

[1] A. Shon, K. Brakel, M. Hook, and H. Park, "Closed-loop plantar cutaneous augmentation by electrical nerve stimulation increases ankle plantarflexion during treadmill walking," *IEEE Transactions on Biomedical Engineering*, vol. 68, no. 9, pp. 2798–2809, 2021.

[2] S. Mabrouk, S. Hersek, H. K. Jeong, D. Whittingslow, V. G. Ganti, P. Wolkoff, and O. T. Inan, "Robust longitudinal ankle edema assessment using wearable bioimpedance spectroscopy," *IEEE Transactions on Biomedical Engineering*, vol. 67, no. 4, pp. 1019–1029, 2019.

[3] T. W. Kaminski and H. D. Hartsell, "Factors contributing to chronic ankle instability: a strength perspective," *Journal of athletic training*, vol. 37, no. 4, p. 394, 2002.

[4] G. L. Lentell, L. L. Katzman, and M. R. Walters, "The relationship between muscle function and ankle stability," *Journal of Orthopaedic & Sports Physical Therapy*, vol. 11, no. 12, pp. 605–611, 1990.

[5] E. Verhagen, A. J. Van der Beek, L. M. Bouter, R. Bahr, and W. Van Mechelen, "A one season prospective cohort study of volleyball injuries," *British journal of sports medicine*, vol. 38, no. 4, pp. 477–481, 2004.

[6] N. Malliaropoulos, M. Ntessalen, E. Papacostas, U. Giuseppe Longo, and N. Maffulli, "Reinjury after acute lateral ankle sprains in elite track and field athletes," *The American journal of sports medicine*, vol. 37, no. 9, pp. 1755–1761, 2009.

[7] M. Knupp, T. H. Lang, L. Zwicky, P. Lötscher, and B. Hintermann, "Chronic ankle instability (medial and lateral)," *Clinics in Sports Medicine*, vol. 34, no. 4, pp. 679–688, 2015.

[8] C. Doherty, C. Bleakley, E. Delahunt, and S. Holden, "Treatment and prevention of acute and recurrent ankle sprain: an overview of systematic reviews with meta-analysis," *British journal of sports medicine*, vol. 51, no. 2, pp. 113–125, 2017.

[9] S. B. Thacker, D. F. Stroup, C. M. Branche, J. Gilchrist, R. A. Goodman, and E. A. Weitman, "The prevention of ankle sprains in sports," *The American journal of sports medicine*, vol. 27, no. 6, pp. 753–760, 1999.

[10] M. J. Callaghan, "Role of ankle taping and bracing in the athlete." *British journal of sports medicine*, vol. 31, no. 2, pp. 102–108, 1997.

[11] K. L. Bennell and P. A. Goldie, "The differential effects of external ankle support on postural control," *Journal of Orthopaedic & Sports Physical Therapy*, vol. 20, no. 6, pp. 287–295, 1994.

[12] S. Gunay, A. Karaduman, and B. Ozturk, "Effects of aircast brace and elastic bandage on physical performance of athletes after ankle injuries," *Acta Orthopaedica et Traumatologica Turcica*, vol. 48, no. 1, pp. 10–16, 2014.

[13] R. Voegeli, J. Heiland, S. Doppler, A. Rawlings, and T. Schreier, "Efficient and simple quantification of stratum corneum proteins on tape strippings by infrared densitometry," *Skin Research and Technology*, vol. 13, no. 3, pp. 242–251, 2007.

[14] J. Blanco-Rivera, J. Elizondo-Rodríguez, M. Simental-Mendía, F. Vilchez-Cavazos, V. M. Peña-Martínez, and C. Acosta-Olivo, "Treatment of lateral ankle sprain with platelet-rich plasma: A randomized clinical study," *Foot and Ankle Surgery*, vol. 26, no. 7, pp. 750–754, 2020.

[15] G. Schaap, G. De Keizer, and K. Marti, "Inversion trauma of the ankle," *Archives of Orthopaedic and Trauma Surgery*, vol. 108, pp. 273–275, 1989.

[16] M. W. Wolfe, T. L. Uhl, C. G. Mattacola, and L. C. McCluskey, "Management of ankle sprains," *American family physician*, vol. 63, no. 1, p. 93, 2001.

[17] C. M. Thalman, T. Hertzell, M. Debeurre, and H. Lee, "The multi-material actuator for variable stiffness (mavs): Design, modeling, and characterization of a soft actuator for lateral ankle support," in *2020 IEEE/RSJ International Conference on Intelligent Robots and Systems (IROS)*. IEEE, 2020, pp. 8694–8700.

[18] C. M. Thalman, T. Hertzell, M. Debeurre, and H. Lee, "Multi-degrees-of-freedom soft robotic ankle-foot orthosis for gait assistance and variable ankle support," *Wearable technologies*, vol. 3, p. e18, 2022.

[19] S. Ham, B. B. Kang, K. Abishek, H. Lee, and W. Kim, "Design and validation of tunable stiffness actuator using soft-rigid combined layer jamming mechanism," in *2023 3rd IEEE International Conference on Soft Robotics (RoboSoft)*. IEEE, 2023, pp. 1–6.

[20] Y.-J. Park, J.-G. Lee, S. Jeon, H. Ahn, J. Koh, J. Ryu, M. Cho, and K.-J. Cho, "Dual-stiffness structures with reconfiguring mechanism: Design and investigation," *Journal of Intelligent Material Systems and Structures*, vol. 27, no. 8, pp. 995–1010, 2016.

[21] H. Lee, H. I. Krebs, and N. Hogan, "Multivariable dynamic ankle mechanical impedance with relaxed muscles," *IEEE Transactions on Neural Systems and Rehabilitation Engineering*, vol. 22, no. 6, pp. 1104–1114, 2014.

[22] H. Lee, P. Ho, M. A. Rastgaar, H. I. Krebs, and N. Hogan, "Multivariable static ankle mechanical impedance with relaxed muscles," *Journal of biomechanics*, vol. 44, no. 10, pp. 1901–1908, 2011.

[23] M. Jiang, *Sliding-layer laminates: a new robotic material enabling robust and adaptable undulatory locomotion*. University of California, San Diego, 2018.

[24] C. P. Witana, S. Xiong, J. Zhao, and R. S. Goonetilleke, "Foot measurements from three-dimensional scans: A comparison and evaluation of different methods," *International Journal of Industrial Ergonomics*, vol. 36, no. 9, pp. 789–807, 2006.

[25] S. Raza, H. Raza, and S. Upadhyay, "Anthropometry of the lateral malleolus," *International Journal of Recent Scientific Research*, vol. 6, no. 6, pp. 4821–4826, 2015.

[26] S. Willwacher, A. Bruder, J. Robbin, J. Kruppa, and P. Mai, "A multidimensional assessment of a novel adaptive versus traditional passive ankle sprain protection systems," *The American Journal of Sports Medicine*, vol. 51, no. 3, pp. 715–722, 2023.

[27] S. M. Zinder, K. P. Granata, S. J. Shultz, and B. M. Gansneder, "Ankle bracing and the neuromuscular factors influencing joint stiffness," *Journal of Athletic Training*, vol. 44, no. 4, pp. 363–369, 2009.

IEEE Robotics and Automation Letters (RA-L) paper, presented at ICRA 2024, Yokohama, Japan. Cite as RA-L paper.